Role of electron temperature in the particddpedestal during pedestal evolution

M. Willensdorfer[a,b], E. Fable[a], E. Wolfrum[a], F. Aumayr[b], R. Fischer[a], F. Reimold[a], F. Ryter[b], the ASDEX Upgrade Team[a]

[a] *Max-Planck-Institut für Plasmaphysik, D-85748 Garching, Germany*
[b] *Institut für Angewandte Physik, TU Wien, A-1040 Vienna, Austria*

Abstract

The effect of electron temperature (T_e) on the edge particle transport in the pedestal is analyzed during the density build-up after the L-H transition. Electron cyclotron resonance heating was used to vary the pedestal temperature during the density evolution between subsequent H-mode phases. Although the pedestal T_e and its gradients could be varied by a factor of 2, almost no change in the edge density evolution is observed within the measurement uncertainties. ASTRA was used to interpret the measurements and to analyze the dependence of the pedestal particle transport on the T_e profile. Thermo-diffusion seems to play a minor role in the pedestal.

Keywords: ASDEX-Upgrade, Edge transport barrier, Particle pinch, L-H transition
PACS: 52.25.Fi, 52.65.-y, 52.55.Fa

1. Introduction

The high confinement mode (H-mode) is characterized by a formation of an edge transport barrier (ETB) in energy and particle transport leading to a pedestal in the edge temperature and density [1]. Understanding the particle transport in the pedestal is particularly important for ITER and other future large scale fusion machines, since it affects the fuelling efficiency and the achievable density [2]. Especially, the non-diffusive particle transport is of interest, because an inwards directed non-diffusive particle transport (particle pinch) would reduce the requirements for fueling within the confined region.

Recent studies analyzed the role of diffusive and convective particle transport in the pedestal during the density build-up following the transition from low confinement mode (L-mode) to H-mode (L-H transition) in ASDEX Upgrade [3]. It was shown that a diffusive ETB is required to explain the density build-up, whereas a possible particle pinch in the pedestal could neither be confirmed nor excluded. But it was possible to estimate an upper bound for such a particle pinch at the edge (5 m/s).

Previous experimental studies of the core and theoretical simulations indicate a dependence of a particle pinch on $\nabla T_e/T_e$, $\nabla q/q$ [4, 5] and collisionality [6]. To gain more information about a possible pinch, we continued the work based on the studies of Ref. [3] and investigated the role of the electron temperature profile on the particle transport in the pedestal.

To investigate a particle pinch and to separate it from the effective diffusion coefficient it is necessary to analyze transient plasma phenomena. Furthermore, the analysis of a temperature dependent edge particle transport during the fully developed H-mode includes some difficulties. Edge kinetic profiles in H-mode are not only determined by transport properties, but also by magnetohydrodynamic instabilities like edge localized modes (ELMs) [7]. Thus, we decided to investigate the effect of the electron temperature profile on the particle transport during the density build-up. For this purpose, we extended the analysis of Ref. [3] to recently conducted experiments, in which the pedestal temperature was varied by a factor of around 2 throughout the density evolution following the L-H transition. In section 2, the experimental setup, the measurements and the modeling are presented. The interpretation of these results are discussed in section 3 and a short conclusion is presented in section 4.

2. Experimental setup and analysis

2.1. Discharge setup

At ASDEX Upgrade [8], we performed experiments with subsequently induced H-mode phases using electron cyclotron resonance heating (ECRH) pulses with different power levels during one discharge [3, 9]. Only ECRH is used to avoid an additional particle source within the confined region. In contrast to the experiments in Ref. [3], a plasma current of 0.8 MA instead of 1 MA was chosen to achieve a longer current flattop phase. Furthermore, we used feed forward gas puffing. Figure 1 shows time traces of three H-mode phases (phase I, II and III) relative to the L-H transition during one discharge (#28125). The time traces of the ECRH power are shown in figure 1(a). The lower ECRH power level was set to 1.8 MW to achieve a relatively fast transition from L-mode to the ELM-free H-mode. The upper ECRH power level was set by the maximum available ECRH power. To isolate the influence of T_e on the density evolution, the same conditions before the L-H transition in all H-mode phases were needed. Hence, the fueling and the time between ECRH pulses were kept constant, which ensured

Email address: matthias.willensdorfer@ipp.mpg.de (M. Willensdorfer)

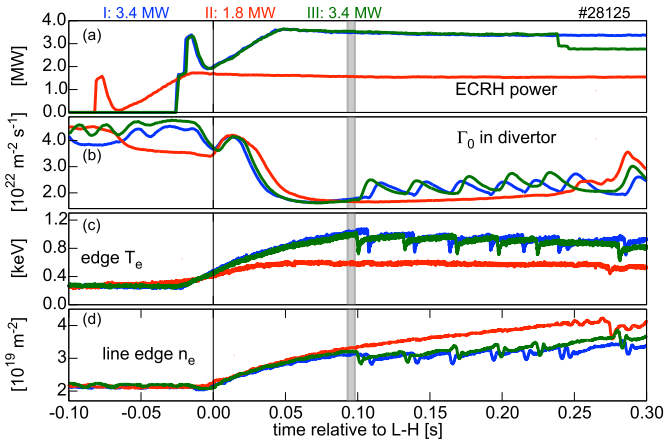

Figure 1: Time traces relative to the L-H transition, which occurred at 2.620 s for phase I, phase II at 3.682 s and phase III at 4.619 s in discharge #28125. (a) ECRH power, (b) neutral flux density in the divertor, (c) edge electron temperature and (d) line integrated density relative to the L-H transition for H-mode phases with different ECRH power. The vertical grey shaded areas indicate the time window for the kinetic profiles shown in figure 2.

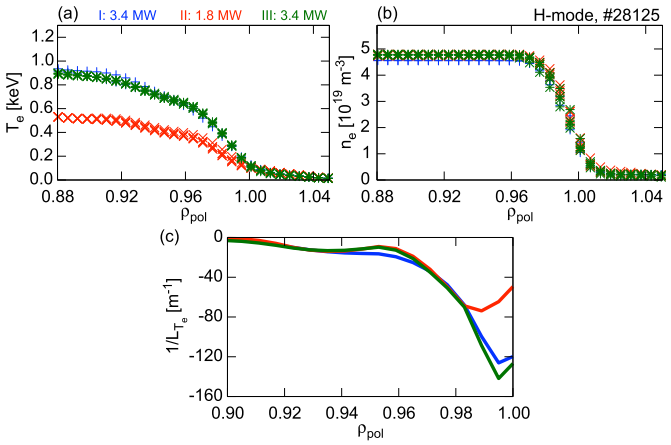

Figure 2: (a) T_e profiles and (b) n_e profiles from IDA in H-mode. Although the edge T_e evolution differs significantly, the n_e profiles evolved identically. (c) The normalized temperature gradient during the three H-mode phases. The used time window for these H-mode profiles are indicated by the grey shaded area in figure 1. In the pedestal, a factor of 2 in the T_e gradient between the high and low power case could be achieved.

similar neutral gas reservoirs prior to the L-H transitions [9]. The neutral gas flux density and its evolution were similar in all H-mode phases and decreased after the L-H transitions (figure 1(b)) [9]. Because of the different heating power levels, T_e evolves differently (figure 1(c)). Although the T_e evolution differed, the density developed identically until the first ELM appeared. In the high power cases, T_e evolves faster and the ELMs appeared earlier. In this case the critical pressure gradient [7], which is a necessary condition for ELMs, is reached earlier. Since these H-mode phases were done within one discharge, the impurity content and wall conditions do not change in-between the different H-mode phases. This is also indicated by the same behavior of phase I and III.

2.2. *Kinetic profiles*

We used integrated data analysis (IDA) [10] to evaluate n_e and T_e profiles. It combines the lithium beam [11] and interferometry diagnostics [12] for n_e profiles. For the evaluation of T_e profiles a new forward modeling of the electron cyclotron radiation transport from the electron cyclotron emission was used [13].

Figure 2 shows the edge electron density and temperature profiles in H-mode during the three H-mode phases (time is indicated by the grey shaded area in figure 1). Prior to the L-H transition the n_e and T_e profiles are almost identical (not shown). But 100 ms after the L-H transition, the T_e profiles (Fig. 2(a)) vary nearly by a factor of 2 at the pedestal top, whereas no differences are seen in the n_e profiles (Fig. 2(b)). To demonstrate that not only the absolute temperature values differ but also the normalized gradients, the normalized gradient $\nabla T_e/T_e = 1/L_{T_e}$ is shown in figure 2(c). The maximal value of the normalized gradient deviates in the pedestal region by a factor of about 2.

2.3. *Modeling*

The experiments show significant differences in the T_e profiles und in their gradients, but almost no differences are seen in the n_e profiles. To interpret these measurements, we simulated the density build-up using the 1.5D fluid code ASTRA [14]. Exactly the same procedure as in Ref. [3] was used. We did extensive parameter scans, in which the diffusion coefficient profiles, the convective velocity profiles and the neutral gas density were varied until the best match with the measured n_e profile was found. We assumed a radially constant core diffusion coefficient ($D = 2.5$ m^2/s). To simulate a diffusive ETB, a variable reduction at the edge (D_{edge}) was added. To account for the observed core density peaking, the v/D ratio in the core was calculated. In combination with the core diffusion coefficient and the fixed v/D ratio, the convective velocity profile in the core was determined. At the edge, a variable increase of the velocity (v_{edge}) was added to simulate a particle pinch. A tanh-function was used to get an analytical expression for the change at the edge in the diffusion coefficient and the convective velocity profile (details in Ref. [3] in Section 3). The particle source profile was calculated using the subroutine NEUT [14]. To scan the particle source profile, we varied the incoming neutral flux for NEUT by varying the incoming neutral gas density n_0, whereas the incoming neutral gas temperature were fixed to 3 eV. A discussion about these assumptions is given in Ref. [3] in Section 5.

At these densities, the plasma is mainly fueled by the neutral gas reservoir from the high field side (HFS) in the divertor [11, 15]. Throughout the density build-up, on one hand the neutral gas density in the divertor decreases but on the other hand the opacity of the scrape off layer (SOL) increases. Due to the lack of information about the neutral gas density distribution and kinetic profiles in the divertor at the HFS, it is not even clear if the neutral gas density at the separatrix either increases or decreases throughout the density build-up. Because of these

uncertainties and to simplify the analysis, we decided to use a time independent incoming neutral flux. Additional to the incoming neutral flux, the particle transport properties were also kept constant in time. For the first simulations, we scanned the edge diffusion coefficient (D_{edge}) from 0.1 to 1 m^2/s , the particle pinch ($v_{edge} \sim 0-5$ m/s) and the incoming neutral flux via the neutral gas density ($n_0 \sim 0 - 4 \cdot 10^{16}$ m^{-3}).

Figure 3 shows the simulations with the lowest deviation between simulations and measurements of H-mode phase III (green in figure 1). First, we assumed a diffusive ETB (D-ETB, blue) and then, a combination of diffusive and convective ETB (v,D-ETB, red). The time traces of the measurements (black) and the simulations throughout the density build-up are shown in figure 3(a). The profiles shortly after the L-H transition are in (b) and in the more developed H-mode phase in (c). The best run was achieved using $D_{edge} = 0.025$ m^2/s, $v_{edge} = -1.5$ m/s and $n_0 = 0.4 \cdot 10^{16}$ m^{-3} and for the case with diffusive ETB only $D_{edge} = 0.075$ m^2/s and $n_0 = 2.1 \cdot 10^{16} m^{-3}$. One should note that compared to the experiments in Ref. [3], these experiments were done at a plasma current of 0.8 MA instead of 1 MA. This reduces the time between the L-H transition and the first ELM and therefore, only the first 100 ms could be analyzed. Furthermore, densities from the simulations and experiments deviates during the initial phase, which is due to the assumption of time independent transport properties as already discussed in Ref. [3]

We applied this analysis method to each H-mode phase and obtained similar particle transport properties. This is already an indication that changes in the T_e profile have a minor impact on the particle transport properties in the pedestal during its evolution.

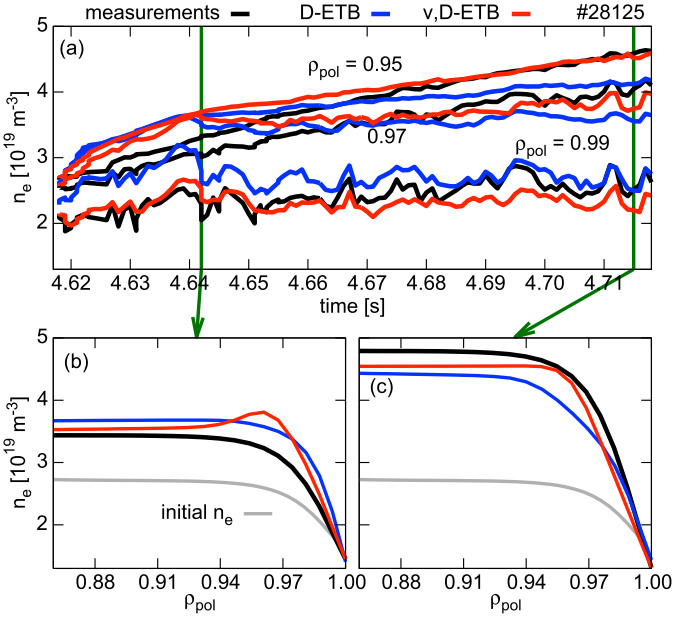

Figure 3: Simulation results using only a diffusive particle ETB (D-ETB) in blue and the combination of convective and diffusive ETB (v,D-ETB) in red. Measurements are in black. (a) Time traces of the measurements and modeling, (b) n_e profiles shortly after the L-H transition and (c) n_e profiles in the more developed H-mode phase.

3. Discussion

The electron temperature or ECRH power can influence the particle transport in the ETB via: (i) The neutral flux across the separatrix because of a change in recycling, (ii) the ionization source due to the T_e dependent rate coefficients, (iii) thermo-diffusion driven by $\nabla T_e/T_e$ and (iv) other T_e dependent transport mechanism, e.g. gyro-Bohm, Bohm diffusion or turbulent transport. In the following, we discuss every point with respect to simulations and experimental measurements.

3.1. Changes in the recycling

Changes in ECRH power not only varies the deposited heating power within the confined region, but also the particle flux towards the target. On one hand, a higher ECRH could lower the particle flux towards the targets due to higher divertor temperatures and lower divertor densities during attached divertor condition. But on the other hand, ECRH power could also lead to an increase of the particle flux due to an increased turbulent transport, which would increase the density. A measure for the particle flux onto the divertor targets is given by the saturation current of the Langmuir probes. According to these measurements, the particle flux during the first 100 ms between phase I and II increased not more than 11.6% and only 1.2% between phase III and II. A change of 11.6% in the incoming neutral flux is not sufficient to have a visible effect on the density evolution. One should also keep in mind that a transient phenomenon was analyzed and because of the newly established ETB, the particle flux towards the first wall and hence, the recycling is generally low during the ELM-free H-mode

3.2. Changes in the ionization

The calculated particle source profile depends on the amount of the incoming neutral flux as well as on the temperature dependent ionization rate coefficients. To test the impact of T_e on the source profile and the density profile evolution, we simply simulated the evolution of the high power case (phase III, Fig. 3) using T_e profiles from the low power case (phase II). All other parameters, e.g. incoming neutral flux, were kept constant. Figure 4 shows (a) the particle source and (b) the evolved density profile 100 ms after the L-H transition. The solid line corresponds to the simulations using the original data and the dashed lines show the simulations using T_e profiles from the low power case. Simulations assuming only a diffusive ETB are shown in blue and the combination of pinch and diffusive ETB in red. These results indicate that lower T_e profiles lead to a deeper penetration of neutrals and hence, to a higher fuelling efficiency. Consequently, the density profiles evolve to higher densities. This difference in the density rise is less pronounced in the simulations using a particle pinch. The addition of a particle pinch requires a lower amount of incoming neutrals to achieve the same pedestal density, which then reduces the influence of the source on the density evolution.

The exchange of the two T_e profiles did not strongly influence the neutral ionization within the pedestal, because of a combination of two effects. Both T_e profiles have a similar separatrix temperature of 100 eV (Fig. 2(a)), which is expected

from the 2-point model [16]. Inside the confined region near the separatrix ($\rho_{pol} \sim 0.99$), where the ionization rate has its maximum, the T_e profiles from the two ECRH power steps start to deviate. Additionally, the ionization rate coefficient has its maximum around 145 eV and shows a slow decay towards higher temperatures [17]. Both facts, similar separatrix temperature and the weak dependence of the ionization inside the separatrix, diminish the effect of the different T_e profiles on the neutral ionization and hence, on the particle source.

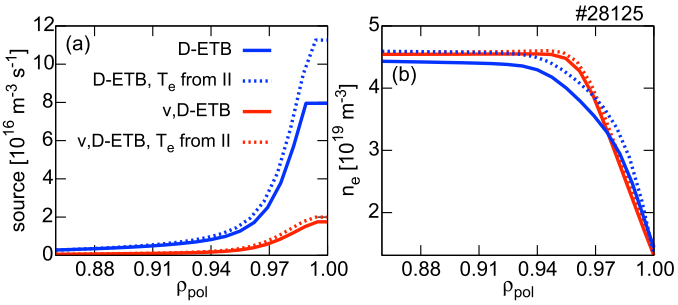

Figure 4: (a) Particle source profile and (b) n_e profile 100 ms after the L-H transition of H-mode phase III simulated with original and lower T_e profiles. A lower pedestal temperature increases the particle source, which results in an evolution to higher densities.

3.3. Thermo-diffusion

In the previous section, it was shown that a higher T_e leads to a smaller neutral penetration depth and therefore, to a lower density in the pedestal. In the experiments almost the same density evolution was observed for different T_e. This could imply that either a particle pinch, which is independent of T_e, exists or an inwards directed thermo-diffusion term is counter-acting the lower fuelling efficiency due to the higher T_e and lower penetration depth of neutrals.

To analyze the role of thermo-diffusion in the density build-up and to estimate its value, we extended the expression for the particle flux Γ from Ref. [3] to

$$\Gamma = -\left\langle \nabla\rho_{pol}^2 \right\rangle D \frac{\partial n}{\partial \rho_{pol}} - \left\langle \nabla\rho_{pol}^2 \right\rangle D_{th} \frac{1}{T_e}\frac{\partial T_e}{\partial \rho_{pol}} n + \left\langle \nabla\rho_{pol} \right\rangle v\, n, \quad (1)$$

where the first term is the usual particle diffusion term, the second is the thermo-diffusion term and the third is the convective term including all other non-diffusive transport process. In comparison to the previous simulations in section 2.3 and Ref. [3], the non-diffusive term is now split into a thermo-diffusion term and a convective term. Unlike the particle diffusion coefficient D, the thermo-diffusion coefficient D_{th} can have positive and negative sign and can contribute as an inwards or outwards directed flux.

To estimate the range for a possible thermo-diffusion coefficient (D_{th}), we assumed that the density evolution is the same despite the T_e profiles or ECRH power. Furthermore, we inferred that the change in the ionization is balanced by the thermo-diffusion. To simplify this analysis, a temporally and radially independent D_{th} was assumed. Although the three H-mode phases showed the same density evolution, the simulations of these phases can slightly differ due to variations in the equilibrium, boundary condition, etc. To have a more consistent comparison of the effect of the temperature on the density build-up, we only analyzed the density evolution of H-mode phase III. In the following, we simulated the density evolution of H-mode phase III, one time using the original data set and one time using the lower T_e profiles from phase II. In addition, D_{th} was scanned between -0.03 and 0.03 m^2/s for both cases. Our approach was that the most reasonable D_{th} is given, when the simulation shows the smallest change in the density evolution despite the chosen T_e profiles (phase II and III) for one D_{th} value.

Figure 5 shows the relative difference of the evolved density at the pedestal top of the H-mode phase III between the calculations using the original T_e and T_e from phase II versus the thermo-diffusion coefficient. This scan was done one time using parameters from the best diffusive ETB simulations (red, D-ETB) and one time from the best combination of convective and diffusive ETB (blue, v,D-ETB, section 2.3). No change in the simulated n_e evolution using the different T_e profiles is seen, when a D_{th} slightly higher than -0.01 m^2/s (-0.013) was applied in the diffusive ETB case. For the combined convective and diffusive ETB simulation only a D_{th} of -0.002 m^2/s is needed. Since the case with diffusive ETB is most sensitive to the particle source, we can roughly estimate from this case an upper limit of $D_{th} \sim -0.01$ m^2/s in the pedestal region. One can estimate the weight of the thermo-diffusion term in comparison to the diffusion term by calculating the ratio between D_{th} and D assuming similar normalized temperature and density gradients. Consequently, the thermo-diffusion term is only 1/7.5 of the diffusion term and hence, plays a minor role.

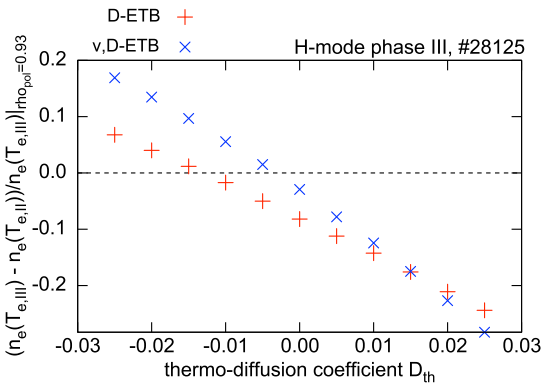

Figure 5: Differences in the evolved density (100 ms after L-H transition) at the pedestal (ρ_{pol} 0.93) of H-mode phase III using T_e profiles from phase II ($T_{e,II}$) and phase III ($T_{e,III}$) over the thermo-diffusion coefficient D_{th}. No difference in the evolution could be observed, if D_{th} of ~ -0.013 m^2/s is added to the diffusive ETB case (D-ETB) and ~ -0.002 m^2/s in the convective and diffusive case (v,D-ETB).

3.4. Other transport mechanism

Various transport mechanism can show a dependence on T_e as well. For example, assuming gyro-Bohm diffusion and

Bohm diffusion one would expect that the diffusion coefficient D increases with $\propto T_e^{3/2}$ and T_e, respectively, which would increase the outwards particle flux. Also the particle flux of turbulent transport can depend on the T_e profile via $\nabla T_e/T_e$ (e.g. trapped electron modes) or indirectly via $\nabla p_e/p_e$ (e.g. drift wave transport). The turbulent particle flux is determined by the cross-phase between density and potential fluctuations. Both described cases would increase the outwards directed particle flux. This would lead to a smaller density gradient and higher particle flux towards the target plates in the divertor in this density range. This was not observed in these dedicated experiments as well as in previous experiments (see Section 3.2 in [9]). Moreover, it is not clear, which mechanism is responsible for the particle transport in the pedestal, since no conclusive study for the pedestal has been done.

4. Conclusions and outlook

We performed experiments to investigate the role of the pedestal temperature on the density build-up after the L-H transition. Because of the different ECRH power steps, we achieved a variation of roughly a factor of 2 in the electron temperature at the pedestal top and in the pedestal T_e gradient throughout the pedestal evolution. Although the T_e profile differs significantly, density measurements show almost no differences in the density profile evolution between the two ECRH power level. Changes in recycling between the two ECRH power steps were small, which is indicated by small changes ($< 11\%$) in divertor probe measurements as well as by small variations in the manometer gauge measurements. Also the variation in the ionization rate in the pedestal between the ECRH steps is small because of the similar separatrix electron temperatures and the characteristics of the ionization rate coefficients (maximum at 145 eV and slow decay towards higher temperatures). Moreover, the fact that the T_e gradients were varied by a factor 2 and almost no change in the n_e profiles and theirs gradients are observed already between the two power levels, suggests a minor role of Thermo-diffusion in the pedestal during its evolution. This is also underlined by modeling using extensive parameter scans (Ref. [3]).

For more conclusive studies, one should also include the temporal change of the incoming neutral flux during the density build-up. This is only useful, when supported by H_α, T_e and n_e measurements in the divertor and appropriate analysis methods to extract the neutral gas density.

References

[1] F. Wagner et al., Physical Review Letters 49 (19) (1982) 1408.
[2] A. S. Kukushkin et al., Journal of Nuclear Materials 415 (1, Supplement) (2011) S497–S500.
[3] M. Willensdorfer et al., Nuclear Fusion 53 (9) (2013) 093020.
[4] X. Garbet et al., Physical Review Letters 91 (2003) 035001.
[5] G. T. Hoang et al., Physical Review Letters 93 (2004) 135003.
[6] C. Angioni et al., Plasma Physics and Controlled Fusion 51 (12) (2009) 124017.
[7] P. B. Snyder et al., Physics of Plasmas 9 (5) (2002) 2037–2043.
[8] U. Stroth et al., Nuclear Fusion 53 (10) (2013) 104003.
[9] M. Willensdorfer et al., Nuclear Fusion 52 (11) (2012) 114026.
[10] R. Fischer et al., Fusion Science and Technology 58 (675–682) (2010).
[11] M. Willensdorfer et al., Review of Scientific Instruments 83 (2) (2012) 023501.
[12] A. Mlynek et al., Nuclear Fusion 51 (2011) 043002 (10pp).
[13] S. K. Rathgeber et al., Plasma Physics and Controlled Fusion 55 (2) (2013) 025004.
[14] G. V. Pereverzev et al., IPP Report 5 (98) (2002).
[15] J. Harhausen et al., Plasma Physics and Controlled Fusion 53 (2) (2011) 025002.
[16] J. Neuhauser et al., Plasma Physics and Controlled Fusion 44 (6) (2002) 855.
[17] H.P. Summers et al., Plasma Physics and Controlled Fusion 48 (263).